Computation of Unsteady Transonic Flows by the Indicial Method

W. F. Ballhaus*
NASA Ames Research Center and Aeromechanics Laboratory, U.S. Army Aviation R&D Command, Moffett Field, Calif.
and
P. M. Goorjian*
Informatics Corporation, Palo Alto, Calif.

The indicial method is investigated for the computation of unsteady transonic force and moment coefficients for use in flutter analyses. This approach has the advantage that solutions for all reduced frequencies for a given mode of motion can be obtained from a single finite-difference flowfield computation. Comparisons of indicial and time-integration computations for oscillating airfoil and flap motions help define limits on the motion amplitude for the applicability of the indicial method to transonic flows. Within these limits, solutions for various motion modes can be superposed to obtain solutions for multiple-degree-of-freedom aeroelastic systems. Also, a simple aeroelastic problem is solved by an alternative approach in which the structural motion and flowfield equations are integrated simultaneously using a time-integration finite-difference procedure.

Introduction

IN transonic flight, small-amplitude oscillations of a body can produce large variations in the aerodynamic forces and moments acting on that body. Furthermore, phase differences between the motion and the resulting forces and moments can be large. These characteristics tend to increase the probability of encountering aeroelastic instabilities, making the transonic regime a sensitive one for aircraft flutter. The object of this work is to describe an efficient method for providing aerodynamic input for flutter analysis in the transonic Mach number range.

Flutter boundaries are usually calculated using the following linear system of equations:

$$[M]\ddot{q}+[C]\dot{q}+[K]q=F(q) \tag{1}$$

where M, C, and K are mass, damping, and stiffness matrices, respectively; q is a vector that is a measure of the structural response; and $F(q)$ is a vector of applied forces. The aerodynamic response to the motion $F(q)$ can be computed in several different ways. For example, Eq. (1) could be integrated in time simultaneously with the governing equations for transonic flow. The airfoil motion and aerodynamic forces would then be free to drive each other. Sample computations of this type are presented subsequently.

To begin with, let us assume that the airfoil motion and the force response are simple harmonic. Substituting the expressions $q(t)=\bar{q}e^{i\omega t}$ and $F(q)=[A]q$ into Eq. (1) leaves

$$[K+i\omega C-\omega^2 M]\bar{q}=[A]\bar{q} \tag{2}$$

The matrix $[A]$ represents the dependence of the aerodynamic forces on the motion of the body. For subsonic or supersonic cases, in which the governing aerodynamic equations are *linear*, these forces are independent of the body shape and the mean aerodynamic conditions. The unsteady component of the solution therefore represents the unsteady motion of a flat plate. Furthermore, the forces corresponding to different types of body motions can be *superposed*, i.e., the resultant aerodynamic force acting on the body can be obtained by summing the effects of each of the different types of motion. The forces for each motion are tabulated as functions of freestream Mach number M_∞ and reduced frequency k.

The equations governing transonic aerodynamics are nonlinear, and the superposition principle cannot be applied so generally. In the transonic case, a more limited form of superposition has been applied recently in which unsteady aerodynamic solutions are given as linear perturbations about nonlinear steady-state solutions. Then, the forces corresponding to different types of body motions can be superposed, and the forces for each motion can be tabulated as functions of M_∞ and k, as in the subsonic and supersonic cases. However, these forces are not independent of either the body shape or the mean aerodynamic conditions, and they are valid only for very small oscillation amplitudes, as shown later.

Three procedures have been developed for obtaining the aerodynamic input $[A]$ for Eq. (2): the time integration, harmonic, and indicial approaches. (For a review of unsteady transonic solution methods, see Ref. 1.) In the *time integration* approach, the unsteady equations of motion are integrated in time for harmonic aerodynamic motions until the transients in the solution disappear and the forces become periodic. There is no linear perturbation assumption in the method itself. However, in computing solutions for the aerodynamics matrix $[A]$, motion amplitudes must be small enough that the force response is linear. The force response is linear if it is harmonic and depends linearly on the motion amplitude.

The *harmonic* approach assumes that the flowfield for some sinusoidal body motion of frequency ω can be expressed in the form

$$\phi(x,y,t)=\phi_0(x,y)+\epsilon\phi_1(x,y)e^{i\omega t}+\epsilon^2\phi_2(x,y)e^{2i\omega t}+\ldots \tag{3}$$

where ϕ is the disturbance velocity potential and ϵ is related to the amplitude of body motion. For purely subsonic or supersonic flows, the sinusoidal motion produces a sinusoidal response in ϕ at the same frequency, and all higher-order terms are zero. This is not true in the transonic case, in which higher harmonic content in ϕ results because the governing equations are nonlinear. However, for $\epsilon \ll 1$, i.e., for very small-amplitude motions, terms of order ϵ^2 or higher can still be neglected, but ϕ_1 now depends on the mean steady-state solution ϕ_0, whereas in subsonic or supersonic cases it does not. The harmonic approach has been used by Ehlers et al.[2,3]

Presented as Paper 77-447 at the AIAA Dynamics Specialist Conference, San Diego, Calif., March 24-25, 1977; submitted April 11, 1977; revision received Sept. 29, 1977.

Index categories: Transonic Flow; Nonsteady Aerodynamics; Computational Methods.

*Research Scientist. Member AIAA.

and Traci et al.[4,5] to solve unsteady transonic small-disturbance equations for unsteady airfoil and rectangular wing motions. It has the advantage that ϕ_1 can be computed using essentially the same well-known finite-difference relaxation algorithms used to compute the mean steady-state solution ϕ_0.

Indicial Approach

For a given motion mode and Mach number, the time-integration and harmonic procedures require a complete flowfield solution for each frequency of interest. This can be a very costly procedure, and this factor has motivated the present effort to investigate the indicial approach as a more efficient alternative. The indicial approach has the advantage that, for a given motion mode and Mach number, only a single flowfield calculation, the *indicial response*, need be performed. The indicial response is the flowfield response to a step change in the given mode of motion, and it is computed using a time-accurate finite-difference scheme. From the indicial response, the solution for all oscillation frequencies can be obtained by evaluating simple integrals (derived later), at a small fraction of the cost of the complete flowfield calculations required by the harmonic approach. The indicial approach, like the harmonic approach, uses superposition and, consequently, for transonic flow applications, unsteadiness must be treated as a small (linear) perturbation about some nonlinear steady-state solution.

If the indicial response to some motion (pitch, plunge, etc.) is known, the solution for any arbitrary schedule of that motion can be found with the aid of Duhamel's integral. For example, consider some arbitrary variation of angle-of-attack α as a function of time (Fig. 1a), and suppose that the lift coefficient response to a change in angle of attack is given as shown in Fig. 2. The motion can be divided into equal $\Delta\alpha$ increments. The value of C_ℓ (Fig. 1b) at some time t is then given by the sum of the increments ΔC_ℓ due to the $\Delta\alpha$ increments. The increments in C_ℓ for the various $\Delta\alpha$ steps at time t are equivalent to increments in the first step (indicated by arrows) at $t-\tilde{t}$, where $\tilde{t}$ is the time at which the corresponding $\Delta\alpha$ is initiated. The total lift at time t is then given by the summation[6]:

$$C_\ell(t) = C_{\ell_\alpha}(t)\alpha(0) + \sum_0^t C_{\ell_\alpha}(t-\tilde{t})\frac{\Delta\alpha}{\Delta\tilde{t}}(\tilde{t})\Delta\tilde{t} \tag{4}$$

where $C_{\ell_\alpha}(t)$ is the indicial response to a unit change in α. Introducing a change of variable and letting the time increment approach zero leaves

$$C_\ell(t) = C_{\ell_\alpha}(t)\alpha(0) + \int_0^t C_{\ell_\alpha}(\tau)\frac{\mathrm{d}}{\mathrm{d}t}\alpha(t-\tau)\,\mathrm{d}\tau \tag{5}$$

Once the indicial response $C_{\ell_\alpha}(t)$ is known, the lift coefficient for any $\alpha(t)$ schedule can be found from Eq. (5). For example, this approach can be used to determine the surface pressures and forces resulting from the sinusoidal oscillation of an aerodynamic configuration.[6] Let the motion be given by

$$\alpha(t) \equiv \alpha_0 + \alpha_1 e^{i\omega t} \tag{6}$$

and define

$$\Delta C_{\ell_\alpha}(\tau) \equiv C_{\ell_\alpha}(\infty) - C_{\ell_\alpha}(\tau) \tag{7}$$

where $C_{\ell_\alpha}(\infty)$ is the steady-state change in lift due to a unit change in α. Then, substituting into Eq. (5) and taking the limit as $t\to\infty$ (since we are only interested in the periodic solution) gives

$$C_\ell(t) = \alpha_1 e^{i\omega t}\left[C_{\ell_\alpha}(\infty) - i\omega\int_0^\infty \Delta C_{\ell_\alpha}(\tau)e^{-i\omega\tau}\mathrm{d}\tau\right] + C_{\ell_\alpha}(\infty)\alpha_0 \tag{8}$$

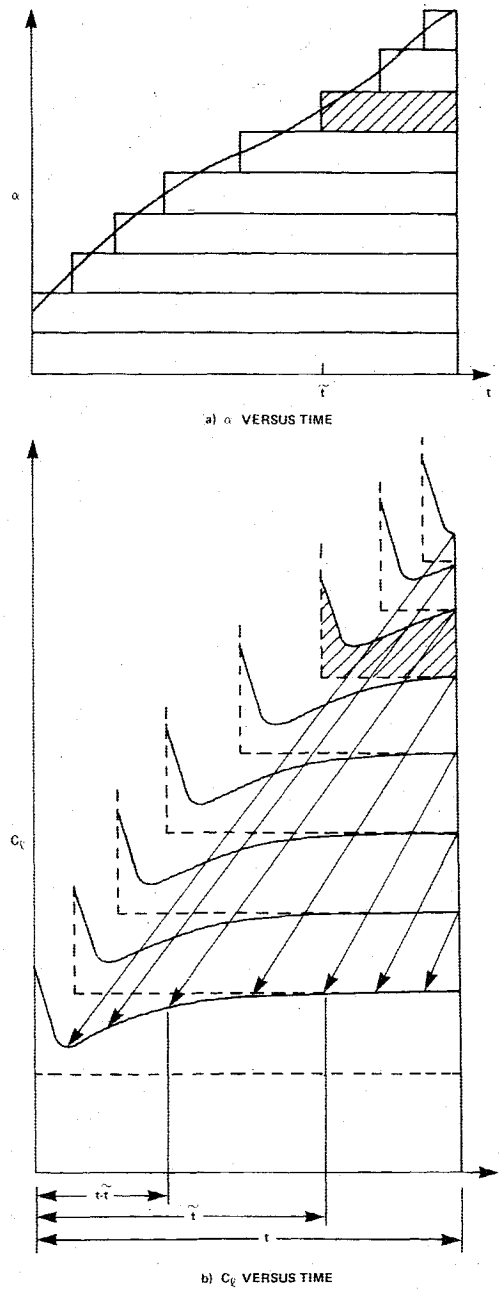

Fig. 1 C_ℓ response for arbitrary angle-of-attack schedule by superposition.

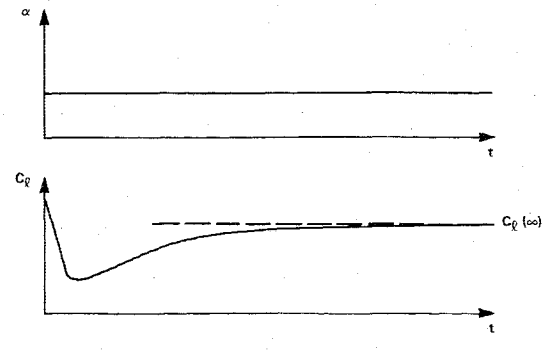

Fig. 2 Indicial C_ℓ response to a step change in angle of attack.

The last term represents the mean steady-state lift and hence the expression for $C_\ell(t)$ has been separated into steady and unsteady components. The solution can be expressed in terms of real and imaginary components as

$$\bar{C}_\ell \equiv \frac{C_\ell - C_{\ell_\alpha}(\infty)\alpha_0}{\alpha_1 e^{i\omega t}} \tag{9a}$$

$$\mathrm{Re}[\bar{C}_\ell] = C_{\ell_\alpha}(\infty) - \omega\int_o^\infty \Delta C_{\ell_\alpha}(\tau)\sin\omega\tau\, d\tau \tag{9b}$$

$$\mathrm{Im}[\bar{C}_\ell] = -\omega\int_o^\infty \Delta C_{\ell_\alpha}(\tau)\cos\omega\tau\, d\tau \tag{9c}$$

In practice, the integrals are evaluated over a finite time interval at least as great as the period of motion considered. Other aerodynamic forces and surface pressures, as well as other types of motion, can all be handled similarly by use of Duhamel's principle.

Governing Equation and Finite-Difference Algorithm

Various forms of governing equations and finite-difference algorithms can be used to compute the indicial response. For example, Beam and Warming[7] obtained solutions by the indicial method using an explicit finite-difference algorithm to solve the unsteady Euler equations. Only parabolic arc airfoils were treated, and boundary conditions were imposed in a small-disturbance fashion on a mean-surface approximation to the airfoil. For more practical airfoils, this procedure would probably not be satisfactory. A more suitable approach would be to use a consistent transonic small-disturbance formulation that would retain the simplified airfoil boundary conditions. For example, one of the algorithms in Ref. 8 could be used to solve the unsteady transonic small-disturbance equation:

$$A\phi_{tt} + 2B\phi_{xt} = C\phi_{xx} + \phi_{yy} \tag{10}$$

where

$$A = k^2 M_\infty^2/\delta^{2/3}$$

$$B = kM_\infty^2/\delta^{2/3}$$

$$C = (1-M_\infty^2)/\delta^{2/3} - (\gamma+1)M_\infty^m\phi_x$$

and where ϕ is the disturbance velocity potential, M_∞ is the freestream Mach number, δ is the airfoil thickness/chord ratio, $k=\omega c/U_\infty$ is the reduced frequency, and the choice of m is somewhat arbitrary.[1] The quantities x, y, t, and ϕ have been scaled by c, $c/\delta^{1/3}$, ω^{-1}, and $c\delta^{2/3}U_\infty$ respectively, where c is the airfoil chord length, ω is the motion frequency, and U_∞ is the freestream velocity. Such an approach would be valid for all reduced frequencies and for $\delta^{2/3} \sim 1-M_\infty^2 \ll 1$. Here, an approximation to Eq. (10), valid for low reduced frequencies, is used, i.e.,

$$2B\phi_{xt} = C\phi_{xx} + \phi_{yy} \tag{11}$$

where B and C are defined in Eq. (10). This equation can be derived from the unsteady Euler equations with the assumptions:

$$k \sim \delta^{2/3} \sim 1-M_\infty^2 \ll 1 \tag{12}$$

We have chosen to restrict the present approach to low reduced frequencies. This frequency range is of primary interest in transonic flow applications. It is not treated efficiently using *explicit* finite-difference algorithms (such as the one used in Ref. 7), which have severe time-step stability restrictions. Here we use the *implicit* finite-difference code LTRAN2[9] to solve Eq. (11). The finite-difference algorithm of LTRAN2 is an alternating-direction implicit (ADI) one for which the integration time step has no restriction for stability that is more severe than that required for accuracy. The ADI scheme was first reported in Ref. 10 and was subsequently adapted to lifting cases and used to compute solutions for several types of unsteady airfoil motions in Ref. 9.

Computed LTRAN2 and exact linear theory lift and moment coefficient indicial responses to step changes in angle of attack are compared in Fig. 3. The comparison is made on a time scale consistent with the low-frequency range. Note that k is given in terms of radians of oscillatory motion per chord length of airfoil travel. The period of oscillation is $2\pi/k$, which, for $k=0.1$ is 62.8 chord lengths of airfoil travel. The linear theory indicial results for Eq. (10) (with $\gamma=-1$) were obtained by Lomax et al.,[11] and the flowfield it simulates adjusts to a step change in angle of attack in the following way: at time zero, the impulsive airfoil sinking motion produces a piston-wave-type, uniform pressure differential that results in a sudden increase in lift. Because the initial pressure differential is uniform, no jump in the pitching moment occurs. The pressure differential is subsequently eroded by waves propagating downstream from the airfoil leading edge. All of this takes place on a time scale much smaller than that associated with the low-frequency theory, for which the downstream propagation rate is infinite.[1,9] Hence no sudden increase or subsequent erosion of lift appears in the low-frequency indicial response, which is a solution to Eq. (11). As time advances, the lift coefficient in both theories increases monotonically toward a common

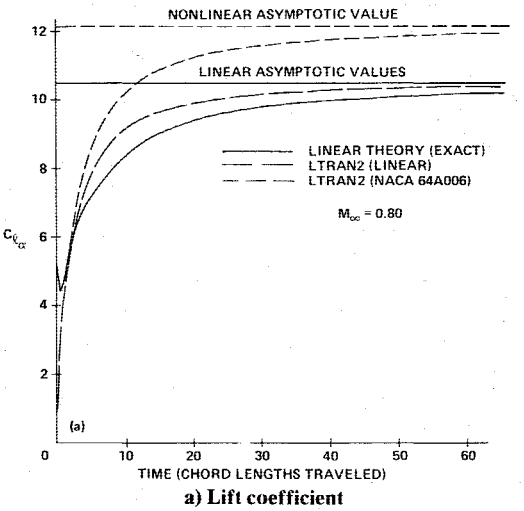

a) Lift coefficient

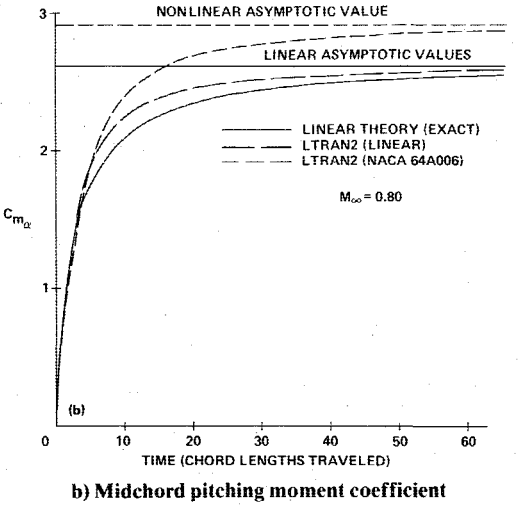

b) Midchord pitching moment coefficient

Fig. 3 Indicial responses to a step change in angle of attack.

steady-state value. The moment coefficient behavior is similar. The indicial response for an NACA 64A006 airfoil is also shown to illustrate the effect of nonlinearity in this case.

For maximum efficiency, an integration time-step schedule should be used that is consistent with the indicial response. Initially, when the flowfield is rapidly adjusting to the step change in the motion, very small time steps should be used. Increasingly larger steps can be taken as the flowfield asymptotically approaches a steady-state condition. Furthermore, the indicial response must be computed over a time interval at least as large as the period corresponding to oscillation frequencies for which oscillatory force coefficients are to be evaluated from Eq. (9).

It should also be mentioned that there exists a maximum reduced frequency that can be treated on a given grid by any finite-difference method. The largest spatial wavelength that can be resolved for a grid spacing Δx is $2\Delta x$. It can be shown that, for upstream-propagating waves to be resolved, the restriction on reduced frequency is $k < \pi(1-M)/\Delta x M$. This restriction also applies to solutions from the indicial method when finite-difference procedures are used to compute the indicial response. Hence, for the treatment of high-frequency motions at Mach numbers near unity, very fine grid spacings must be used. This high-frequency limitation should not be encountered in the present approach, however, which already has a more severe constraint on reduced frequency, Eq. (12).

Some assessment of the computational efficiency of the indicial method can be made relative to the two alternative finite-difference procedures for computing unsteady transonic flow solutions—the *harmonic* approach and the *time-integration* approach. The harmonic and time-integration approaches require complete flowfield computations for each combination of motion mode, Mach number, and frequency of interest. The indicial method requires flowfield computations only for each combination of motion mode and Mach number. Solutions for a large number of frequencies can be computed at a cost slightly greater than for computing only one. The question of relative efficiency, then, depends on 1) the number of frequencies to be computed and 2) the relative costs of flowfield computations for the three procedures. Typically, 200-400 time steps are required with the time-integration approach for a fine (spatial) grid computation. An equivalent or slightly larger number would be required with the harmonic approach. For the indicial response computations (as shown later in Fig. 6), 1200 time steps were used. Note that this excessive number of steps for the indicial approach could probably have been substantially reduced in the following way. Since, in this work, we are concerned only with low-frequency motions, it is not necessary to compute indicial responses to step changes in motion, which contain all frequencies. We could instead have computed responses to motions that changed smoothly from one state to another in a finite time interval. This would permit use of substantially larger initial time steps, thereby reducing the overall number of time steps required. However, it would require the derivation of new equations equivalent to Eq. (9) to obtain oscillatory force coefficients.

Effect of Frequency

Linear time-integration LTRAN2 solutions of the low-frequency Eq. (11) for plunging airfoil oscillations were compared with exact solutions to the linear form of Eq. (10) in Ref. 9. (The linear form of both equations is obtained by taking $\gamma = -1$ in C.) One comparison was made in terms of lift and midchord moment coefficients, normalized by the oscillation amplitude, as functions of reduced frequency for several freestream Mach numbers. The time-integration solutions were obtained by starting with a mean steady-state solution and integrating in time until the solution became periodic. The comparisons generally were favorable for $k \leq 0.2$.

We begin by making a similar comparison in Fig. 4. Here the results from the indicial approach are compared with the LTRAN2 time-integration results of Ref. 9. The comparison serves to check the numerical accuracy in the computation of the indicial response and the evaluation of the integrals in Eq. (9). The plunging airfoil oscillation is $\alpha = \alpha_0 \sin\omega t$, and the lift and moment coefficient responses are $C_\ell = \alpha_0 |C_\ell| \sin(\omega t - \phi_\ell)$ and $C_m = \alpha_0 |C_m| \sin(\omega t - \phi_m)$. Note that the linear time-integration and indicial results agree very well.

In the linear case, the normalized C_ℓ and C_m responses are independent of amplitude and mean steady-state condition. They are also independent of airfoil shape. In the nonlinear case ($\gamma = 1.4$), this is not true, as indicated by the differences between the solutions for the NACA 64A006 and the NACA 64A010 airfoils. This illustrates the inadequacy of the purely linear (or "flat-plate") theory in the transonic regime. Comparison of the NACA 64A006 results at $M_\infty = 0.8$ (Fig. 4a) and $M_\infty = 0.85$ (Fig. 4b) indicates that the influence of the airfoil shape becomes more significant as the flowfield becomes more supercritical. The NACA 64A010 results at $M_\infty = 0.85$ are not shown because the shock waves in that case were so strong that the inviscid and small-disturbance assumptions under which the theory is derived are violated; consequently, the results are physically meaningless.

It is clear from the results in Fig. 4 that the effect of increasing frequency on the lift and moment is to decrease their amplitude and increase their phase lag relative to the motion. This is true, at least in the Mach number range 0.8-0.85 and for reduced frequencies less than 0.2.

Effect of Freestream Mach Number

Figure 5a illustrates the variation of midchord pitching-moment coefficient, normalized by the oscillation amplitude, as a function of freestream Mach number for a reduced frequency of 0.1. The motion is plunging oscillations of an NACA 64A006 airfoil. The "linear" results are LTRAN2 solutions to the linear form of Eq. (11). They show a weak

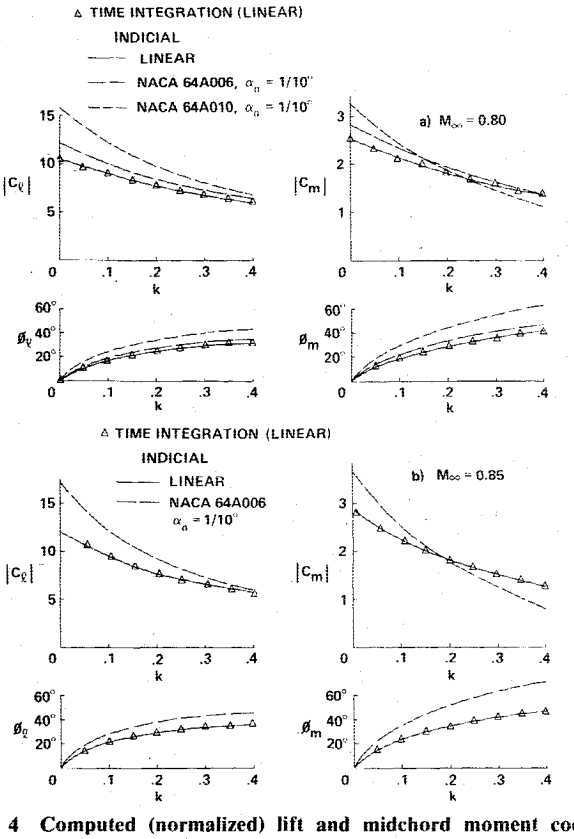

Fig. 4 Computed (normalized) lift and midchord moment coefficients (amplitude and phase) vs reduced frequency for an oscillatory plunging airfoil $\alpha = \alpha_0 \sin\omega t$, $k = \omega c/U_\infty$.

dependence of C_m on M_∞. The nonlinear results were computed using LTRAN2 by starting with a mean steady-state solution and computing until a periodic solution was obtained. Nonlinear moment coefficients show a strong dependence on M_∞. They also depend strongly on oscillation amplitude for higher Mach numbers. This is an indication of nonlinear unsteady behavior, and it is a result of shock-wave motion. The higher amplitude and Mach number pitching-moment variations were also found to be nonsinusoidal in time, a further indication of nonlinear behavior resulting from shock-wave motion.

Pitching-moment coefficients computed using the indicial method are shown in Fig. 5b. Recall that application of the indicial method to transonic flows requires that unsteady effects be treated as linear perturbations about some nonlinear steady-state solution. Hence the indicial results are compared with the time integration $\alpha_0 = \frac{1}{4}$-deg results in Fig. 5a, for which the amplitude is sufficiently small that the linear perturbation assumption is valid. (The good agreement in Fig. 5a between the ¼-deg and ½-deg amplitude cases is a good indication that this is true.)

An important consideration in computing indicial solutions for transonic flows is that the amplitude of the step change in the motion be sufficiently small that shock-wave locations remain essentially fixed. For the lower values of M_∞ in Fig. 5b, a step change of ¼-deg was sufficiently small. For the higher Mach numbers, a smaller step change, $\alpha = 1/10$ deg, was required. The effect of step size on C_m is indicated by the results shown for $M_\infty = 0.86$. Lift- and moment-coefficient indicial responses for two of these amplitudes, $\alpha = \frac{1}{4}$ deg and 1 deg, are illustrated in Fig. 6. The differences are substantial, and this accounts for the differences in the indicial C_m results for the two amplitudes in the plunging airfoil oscillation example in Fig. 5b.

The change in upper-surface shock location as a function of reduced frequency for some of the cases shown in Figs. 5b and 6 for $M_\infty = 0.86$ is illustrated in Fig. 7. Note that the indicial response computation corresponds to $k = 0$. The ¼-deg-amplitude step change in α produces a 5.5% chord change in shock location. For the ½-deg case, the corresponding Δx_s is 13%; for the 1-deg case, the shock moves 29.5% chord to a point very near the airfoil trailing edge. The comparison in Fig. 5b illustrates that, in the particular case considered, a 5.5% change in shock location is permissible and that a change of 13% or larger is not. Of course, the permissible shock displacement also depends on shock strength. The shock motion amplitude for a given oscillation amplitude decreases with k (as shown).

Oscillating Flap Case

From experimental observations[12] of transonic flow about an NACA 64A006 airfoil with a sinusoidally oscillating trailing-edge flap, three types of shock-wave motions have been defined: 1) type A, sinusoidal shock-wave motion, 2) type B, interrupted shock-wave motion, and 3) type C, upstream propagating shock waves. Solutions for the oscillating flap have also been computed using LTRAN2,[9] and the same types of shock-wave motion were observed. Lift and moment

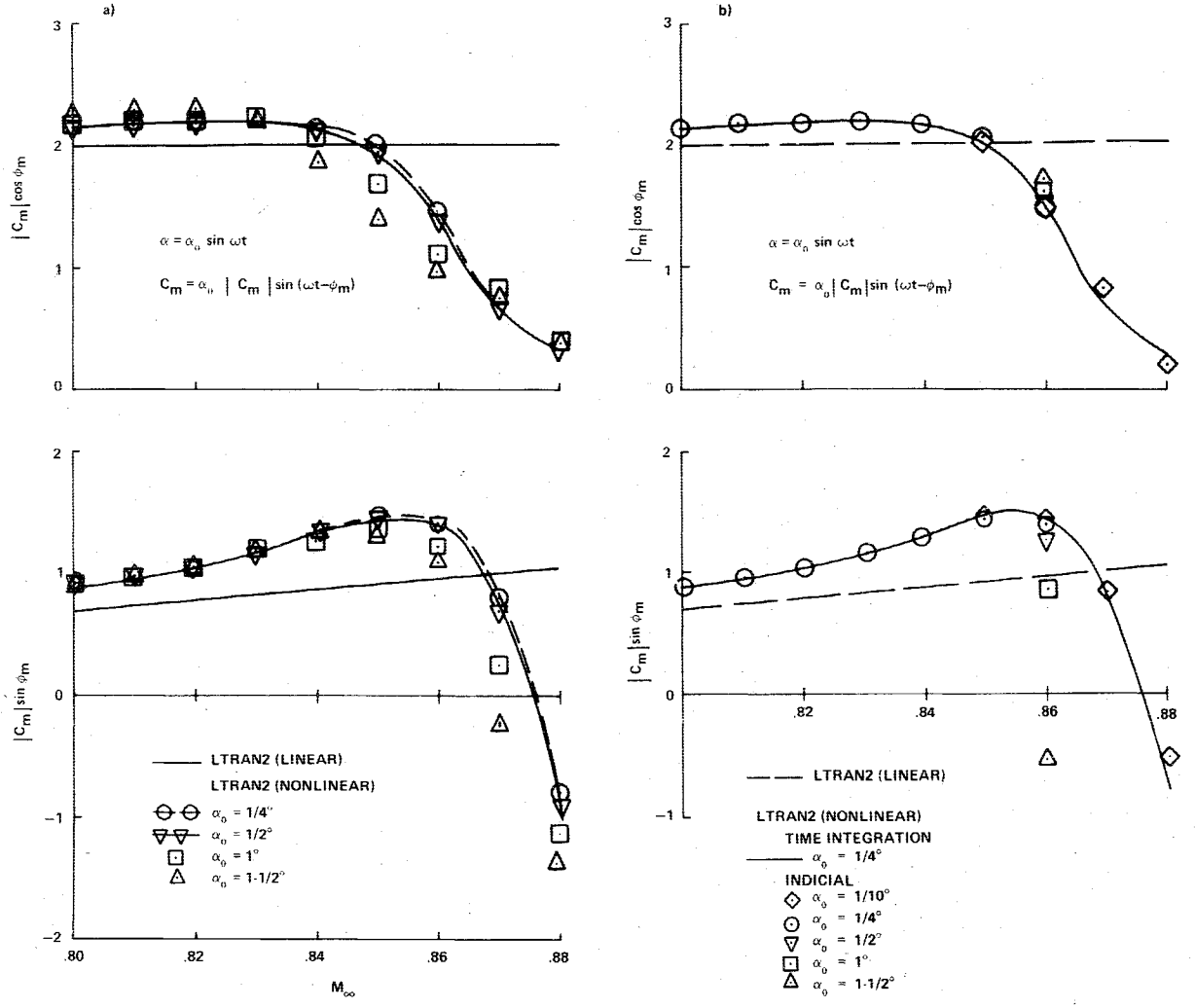

Fig. 5 Midchord moment coefficients vs freestream Mach number for an oscillatory plunging NACA 64A006 airfoil $\alpha = \alpha_0 \sin\omega t$, $k = \omega c/U_\infty = 0.1$: a) time-integration computations, b) indicial calculations.

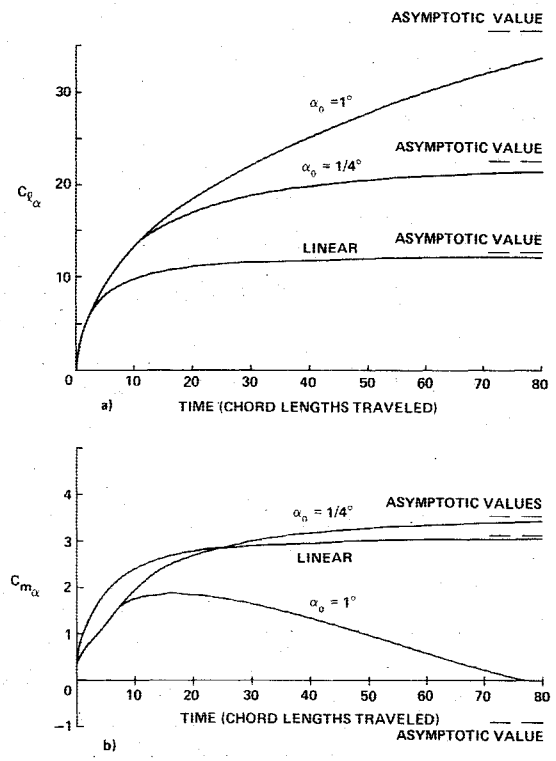

Fig. 6 Responses to step changes in angle of attack (α_θ) for an NACA 64A006 airfoil at $M_\infty = 0.86$: a) indicial lift-coefficient response, b) indicial midchord moment coefficient response.

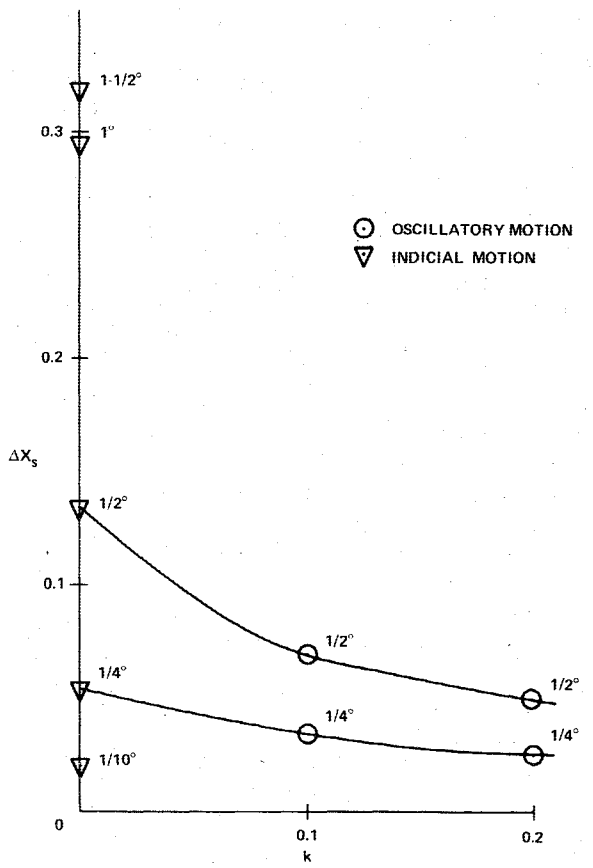

Fig. 7 Change in upper-surface shock location (Δx_s) vs reduced frequency; $k = \omega c/U_\infty$, $M_\infty = 0.86$.

coefficients for these cases are computed with results generated by the indicial method in Fig. 8. The worst agreement between the two solutions is for the type A motion, with the strongest shock waves. In the type B and C cases, for which the shock motion is nonsinusoidal, the indicial and time-integration solutions compare favorably because the shock waves are sufficiently weak that the linear perturbation assumption is a good approximation. No attempt has been made here to compare computed and experimental forces and moments because of anticipated substantial discrepancies caused by viscous and wind-tunnel-wall-interference effects.

Simple Aeroelastic Computations

Here we solve Eq. (1) for single-degree-of-freedom cases in which the motion is not necessarily sinusoidal. Consider an NACA 64A006 airfoil with moment of inertia I free to pitch about midchord. The pitching motion is restricted by a torsion spring of stiffness K and structural damping g. The governing equation is

$$I\ddot{\alpha} + g\dot{\alpha} + K\alpha = M(\alpha) \tag{13}$$

where $M(\alpha)$ is the aerodynamic moment and I, g, and K are all positive constants.

We can construct a neutrally stable system (i.e., a system that will flutter) by properly choosing the structural constants. For example, from an indicial method computation for $M_\infty = 0.88$ and $k = 0.1$, we obtain $|C_{m_\alpha}| = 0.8617$ and $\phi = -68.87$ deg. Assuming the motion can be expressed in the form $\alpha = \alpha_0 e^{i\omega t}$ and substituting this into Eq. (13) results in two expressions [the real and imaginary parts of Eq. (13)] relating the aerodynamic and structural constants:

$$A_1 = -A_3 |C_{m_\alpha}| \sin\phi \tag{14a}$$

$$A_2 = I + A_3 |C_{m_\alpha}| \cos\phi \tag{14b}$$

where

$$A_1 = g/I\omega = 1.072$$

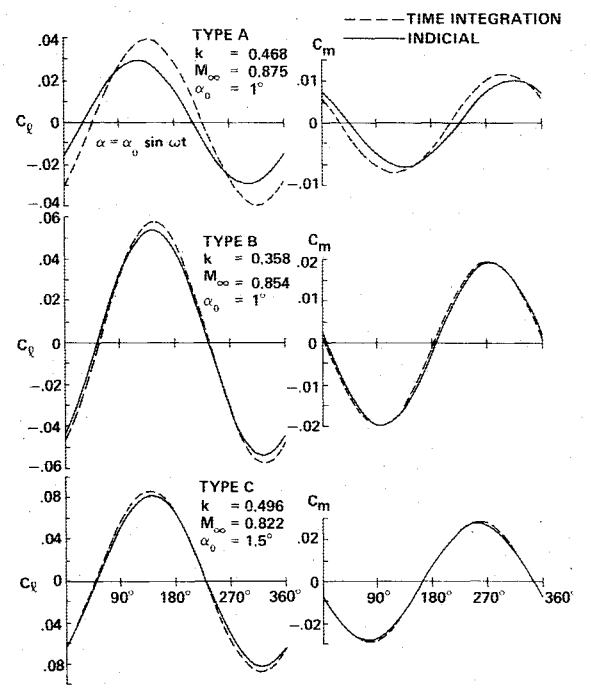

Fig. 8 Comparison of indicial and time integration solutions for an airfoil with oscillating trailing-edge flap.

$$A_2 = K/I\omega^2 = 1.414$$

$$A_3 = qc^2/I\omega^2 = 1.333$$

q = dynamic pressure

The equations are satisfied for the values shown.

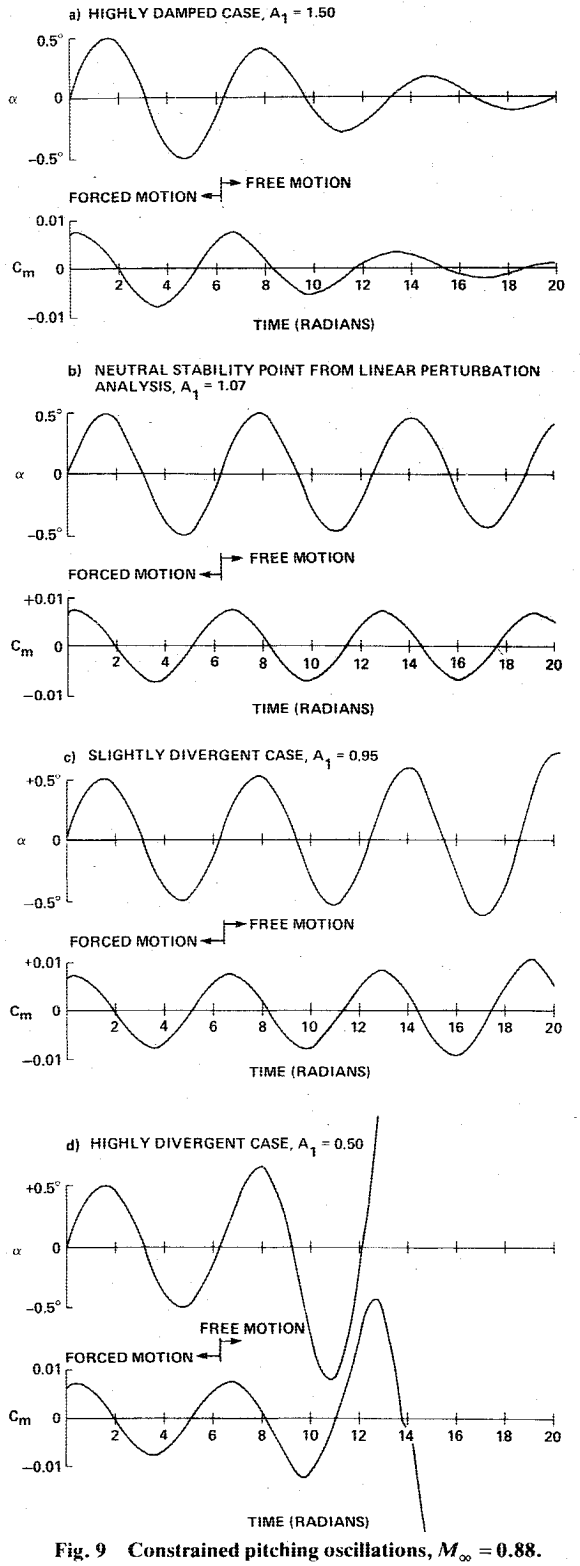

Fig. 9 Constrained pitching oscillations, $M_\infty = 0.88$.

Figure 9 shows aeroelastic responses for a series of computations in which the structural damping A_1 was varied parametrically. These computations were obtained using LTRAN2 coupled with a simple ordinary differential equation integration procedure for Eq. (13). The aerodynamic and airfoil motion equations were integrated simultaneously. The motion was forced for the first few cycles until the pitching moment became periodic, after which the airfoil motion and aerodynamic response were left free to drive each other. The first cycle shown in Fig. 9 is forced for all cases. The initial motion amplitude is $\alpha_0 = \frac{1}{2}$ deg. For $A_1 = 1.072$, i.e., the neutral stability point obtained from the indicial

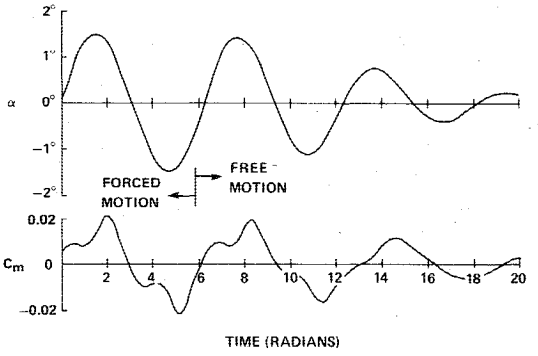

Fig. 10 Constrained pitching oscillations, $M_\infty = 0.87$.

method and Eq. (13), the motion is very nearly sinusoidal. The small deviations from sinusoidal behavior can be attributed primarily to nonlinear unsteady effects and truncation errors in the numerical integration schemes. For other choices of A_1, the motion is either damped or unstable for values greater than or less than the value corresponding to the neutral stability (flutter) point. For this system to flutter, it is necessary that the moment variation *lead* the motion, which it does in the nonlinear case for $M_\infty \geq 0.88$. Linear (flat-plate) theory does not predict a phase lead and thus could not be used in this case to predict the flutter point.

A similar calculation is shown in Fig. 10. The initial amplitude in this case is considerably larger, $\alpha_0 = 1\frac{1}{2}$ deg, and the Mach number is smaller, $M_\infty = 0.87$; the structural constants differ from those in the previous case. This example is presented mainly to illustrate the nonsinusoidal pitching-moment behavior that can result from the large shock-wave excursions encountered at larger airfoil motion amplitudes.

The aeroelastic computations presented here demonstrate that the nonlinear aerodynamic equations and the equations governing the motion of a structure can be integrated simultaneously to provide solutions to aerodynamic problems. The further development of the simultaneous integration approach may eventually lead to the development of computational aeroelastic models from which flutter boundaries could be predicted in a manner similar to existing experimental methods, i.e., the structural model could be perturbed and the response surveyed for disturbances that produce instabilities. Such an approach† might prove advantageous for systems with many degrees of freedom, for which multiple indicial response computations would otherwise be required.

Concluding Remarks

Three procedures have been proposed in recent years for using finite-difference methods to compute unsteady aerodynamic coefficients for use in flutter analyses in the transonic Mach number range: 1) the *time-integration* approach, in which the equations of motion are integrated in time for oscillatory aerodynamic motions until the force responses become periodic, 2) the *harmonic* approach, in which the unsteady component of the solution, assumed to be harmonic, is computed using standard transonic relaxation procedures, and 3) the *indicial* approach, in which solutions are computed using Duhamel's principle and the indicial response. The harmonic and time-integration approaches require the computation of complete flowfield solutions for each frequency, as well as for each Mach number and motion mode of interest. The indicial approach has the advantage that unsteady aerodynamic coefficients for a wide range of frequencies can be simply and efficiently computed from a single flowfield computation—the indicial response. Indicial responses must be computed for each Mach number and

†Suggested to us by James Olsen, Air Force Flight Dynamics Laboratory.

motion mode of interest. Aerodynamic responses to multiple-degree-of-freedom motions can then be obtained by superposition.

For aeroelastic systems with many degrees of freedom, it may eventually prove more efficient to determine flutter boundaries by integrating the equations of motion for the structural motion and aerodynamic response simultaneously instead of by superposing the effects of each of the modes computed independently. Very preliminary computations for a simple aeroelastic problem are reported here to demonstrate that the aerodynamic and structural motion equations can be integrated simultaneously.

References

[1]Ballhaus, W. F., "Some Recent Progress in Transonic Flow Computations," *VKI Lecture Series: Computational Fluid Dynamics*, von Kármán Institute for Fluid Dynamics, Rhode-St-Genese, Belgium, March 15-19, 1976.

[2]Ehlers, F. E., "A Finite-Difference Method for the Solution of the Transonic Flow Around Harmonically Oscillating Wings," NASA CR-2257, 1974.

[3]Weatherill, W. H., Sabastian, J. D., and Ehlers, F. E., "On the Computation of the Transonic Perturbation Flowfields Around Two- and Three-Dimensional Oscillating Wings," AIAA Paper 76-99, Jan. 1976.

[4]Traci, R. M., Farr, J. L., and Albano, E. D., "Perturbation Method for Transonic Flow About Oscillating Airfoils," AIAA Paper 75-877, June 1975.

[5]Traci, R. M., Albano, E. D., and Farr, J. L., "Small-Disturbance Transonic Flows About Oscillating Airfoils and Planar Wings," Air Force Flight Dynamics Laboratory, AFFDL-TR-75-100, June 1975.

[6]Tobak, M., "On the Use of the Indicial Function Concept in the Analysis of Unsteady Motions of Wings and Wing-Tail Combinations," NACA Rept. 1188, 1954.

[7]Beam, R. M. and Warming, R. F., "Numerical Calculations of Two-Dimensional, Unsteady Transonic Flows with Circulation," NASA TN D-7605, 1974.

[8]Ballhaus, W. F. and Lomax, H., "The Numerical Simulation of Low Frequency Unsteady Transonic Flow Fields," *Lecture Notes in Physics*, Vol. 35, Springer-Verlag, Berlin, 1975, pp. 57-63.

[9]Ballhaus, W. F. and Goorjian, P. M., "Implicit Finite-Difference Computations of Unsteady Transonic Flows About Airfoils, Including the Treatment of Irregular Shock-Wave Motions," AIAA Paper 77-205, Jan. 1977; to appear in *AIAA Journal*, Vol. 15, Dec. 1977.

[10]Ballhaus, W. F. and Steger, J. L., "Implicit Approximate-Factorization Schemes for the Low-Frequency Transonic Equation," NASA TM X-73,082, 1975.

[11]Lomax, H., Heaslet, M. A., Fuller, F. B., and Sluder, L., "Two- and Three-Dimensional Unsteady Lift Problems in High-Speed Flight," NACA Rept. 1077, 1952.

[12]Tijdeman, H., "On the Motion of Shock Waves on an Airfoil with Oscillating Flap," *Symposium Transsonicum II*, Springer-Verlag, Berlin, 1975, pp. 49-56.